This paper describes objective technical results and analysis. Any subjective views or opinions that might be expressed in the paper do not necessarily represent the views of the U.S. Department of Energy or the United States Government.

SAND2021-10196J

Improved forward voltage and external quantum efficiency scaling in multi-active region III-nitride LEDs

Zane Jamal-Eddine[1], Brendan P. Gunning[3], Andrew A. Armstrong[3], and Siddharth Rajan[1,2]

[1] Department of Electrical and Computer Engineering, The Ohio State University, Columbus, Ohio, 43210, USA

[2] Department of Materials Science and Engineering, The Ohio State University, Columbus, Ohio, 43210, USA

[3] Sandia National Laboratories, Albuquerque, New Mexico 87185, USA

[a)] Author to whom correspondence should be addressed. Electronic mail: jamal-eddine.1@osu.edu

Abstract

Ultra-low voltage drop tunnel junctions were utilized to enable multi-active region blue LEDs with up to 3 active regions in a single device. The tunnel junction-enabled multi-active region blue LEDs were grown monolithically by MOCVD without growth interruption. Voltage scaling that follows the number of junctions was observed along with external quantum efficiency scaling close to the number of junctions. This work demonstrates that with proper tunnel junction design, it is possible to achieve improvements in wall-plug efficiency at high output power operation by cascading multiple III-Nitride based LEDs grown entirely by MOCVD.

Keywords: tunnel junction, cascaded LED, gallium nitride, blue light emitting diode, tunnel junction optoelectronics, heterojunction tunnel junction, multi-active region LED

Introduction

GaN light emitting diodes (LEDs) have had great success in their applications for high efficiency solid-state lighting. Peak wall-plug-efficiency (WPE) as high as 84% has been reported previously for blue LEDs operating at low current density.[1] There is still substantial interest in high power density III-Nitride visible emitters that could enable several new applications and reduce cost in a variety of existing lighting applications such as domestic, industrial, and automotive lighting.[2] However, due to the problem with efficiency droop in visible III-nitride emitters, which results in a drop in efficiency

Sandia National Laboratories is a multimission laboratory managed and operated by National Technology & Engineering Solutions of Sandia, LLC, a wholly owned subsidiary of Honeywell International Inc., for the U.S. Department of Energy's National Nuclear Security Administration under contract DE-NA0003525.

under high power/current density operation, it has remained challenging to achieve high power density LEDs.[3,4] The efficiency droop problem is one of the key unsolved issues for visible GaN LEDs, but multi-active region LEDs, consisting of identical LED active regions and tunnel junctions (TJ), can provide an elegant solution to circumvent this challenge and enable high power emitters which operate at low current density.[5]

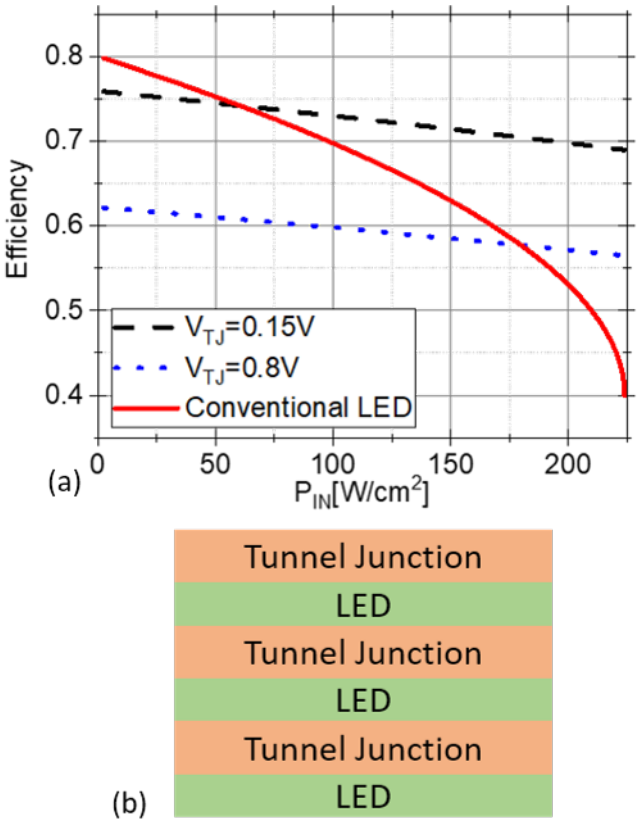

Fig. 1 (a) Modeled efficiency of a conventional LED (red solid line), triple junction LED with 0.15 V TJ loss (black dashed line) which is representative of a triple junction device with state-of-the-art tunnel junctions with low tunnel junction voltage loss, and 0.8 V TJ loss TJ (blue dotted line) which is representative of a triple junction device with previously reported tunnel junction voltage loss, versus input power. **(b)** A schematic showing the device structure of a triple junction cascaded LED.

Figure 1 shows the modeled efficiency of a 3-junction light emitting diode, with realistic efficiency droop parameters similar to current state-of-art LEDs,[2] and a voltage loss at each tunnel junction (V_{TJ}) . In this model, we assumed that the efficiency drops linearly with driving current and that the voltage loss across the tunnel junctions is constant. In reality, the voltage loss across the tunnel junction will

scale with driving current as well, which is why we have chosen tunnel junction voltage loss representative of a tunnel junction operating at high current density (100A/cm2) which will over estimate tunnel junction voltage loss at lower operating currents. This calculation indicates that if tunnel junction voltage losses are sufficiently low, considerably higher efficiency can be achieved in multiple active region LEDs when compared with single-active region LEDs. For example, for a voltage loss per tunnel junction of 0.15, the cascaded structure outperforms the conventional LED above input powers of 70 W/cm^2.

Tunnel junctions grown by molecular beam epitaxy (MBE) have demonstrated sufficiently low voltage loss.[6,7,7,8] However, MBE-grown LED active regions typically suffer from significantly lower EQE. Metal-organic chemical vapor deposition (MOCVD) is the preferred growth method for realizing III-Nitride LEDs, as it offers high quality active regions as well as high throughput for manufacturing. Even with their higher TJ voltage loss, TJ-enabled optoeletronic structures have been grown by MOCVD and have shown a variety of benefits. TJ based VCSELs,[9] high efficiency LEDs with reduced efficiency droop,[10],[11],[12] and MOCVD grown TJ-UVLEDs have all been demonstrated.[13] Howver, efficient, multi-active region LEDs grown by MOCVD had until now not been demonstrated because of the high voltage loss observed in MOCVD-grown GaN-based TJs.[14],[15] Previous demonstrations of multi-active region LEDs grown by MOCVD have shown improvement in EQE but had high TJ voltage losses, which prohibits improvements in WPE over conventional LEDs.[16,17,18] Although a significant reduction in TJ voltage loss can be achieved in MOCVD grown TJs by taking advantage of high In mole fraction heterostructures, there is concern about optical absoprtion in the TJ layers when utilizing such TJ design in a cascaded LED structure.[19] It has been shown that some reduction in forward voltage can be achieved in MOCVD-grown TJs using growth interruptions that enable sharper doping profiles.[20,21] Through improvements in doping scheme and graded heterostructure design, visible-transparent MOCVD tunnel junctions with ultra-low voltage tunnel junctions (0.17 V at 100 A/cm^2) were recently reported.[22] In this work, we show that the state-of-art III-Nitride tunnel junction technology enables 2- and 3-junction cascaded visible LEDs with near-ideal voltage and EQE scaling, as well as improved wall-plug efficiency over a single junction LED.

Methods

The TJ-enabled multi-active region LED devices were grown by MOCVD. Single-junction, two-junction, and three-junction LEDs (Fig. 2(a-c)) were grown. Each device was grown in a single continuous growth run and comprised repetitions of identical LED/TJ stacks (Fig. 2(d)), consisting of an LED multi quantum well (MQW) active region followed by a low-composition graded InGaN TJ. A peak In mole fraction of x=0.06 was chosen such that the TJs remain transparent to the light emitted by the MQW active region. The TJ was designed to reduce its forward voltage significantly. Extensive discussion of the TJ design and MOCVD growth technique used here is presented in our prior work.[22]

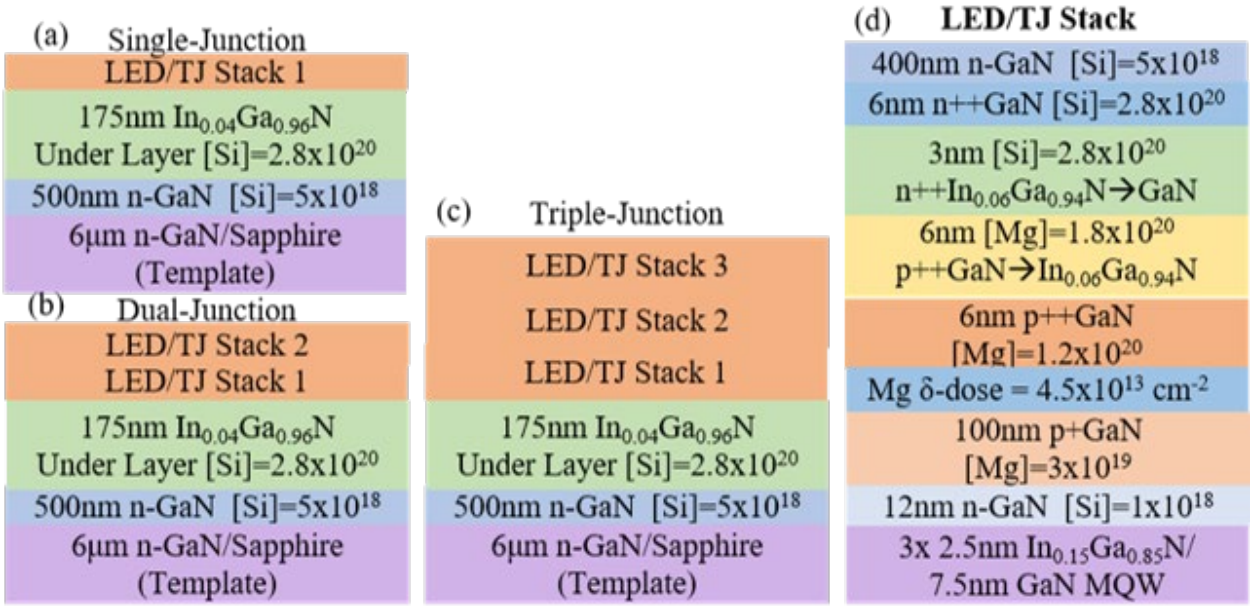

Fig. 2 The epitaxial structure of the **(a)** single junction, **(b)** dual junction, and **(c)** triple junction device. **(d)** The detailed epitaxial structure of each LED/graded InGaN TJ period which comprises the multi-junction cascaded LEDs.

All MOCVD growth in this report was performed at atmospheric pressure in a Taiyo Nippon Sanso SR4000HT reactor. The substrates were ~6um thick n-type GaN/sapphire c-plane templates with typical dislocation density of ~10^8 cm^{-2}. Each structure began with 500nm of n-GaN with [Si]=$5x10^{18}$ cm^{-3} grown at 950°C. Next a 190nm thick $In_{0.04}Ga_{0.96}N$ underlayer was grown at 900°C to prevent the formation of V defects.[23] After the under layer was grown, the LED/TJ stack was grown, 1, 2, or 3 times for the different cascaded structures. The LED/TJ stack begins with the MQW active region consisting

of three sets of 2.5nm thick $In_{0.15}Ga_{0.85}N$ quantum wells with 7.5nm thick GaN barriers, except for the final barrier, which is 12nm thick, all grown at 810°C. Next 100nm of p-GaN with [Mg]=$3x10^{19}$ cm^{-3} was grown at 900°C. The TJ growth begins with a magnesium delta-dose doping equivalent to $4.5x10^{13}$ cm^{-2} inserted at the beginning of the p++GaN layer of the TJ as indicated by the blue box in Fig. 2(d). Then, a 6 nm p++GaN layer with [Mg]=$1.2x10^{20}$ cm^{-3}, followed by a 6 nm thick p++ graded InGaN interlayer with [Mg]=$1.8x10^{20}$ cm^{-3} was grown graded from GaN at the bottom of the layer to $In_{0.07}Ga_{0.93}N$ at the top of the layer. These two p++ (In)GaN layers form the p-side of the TJ. Next, a 3 nm thick n++ graded InGaN interlayer with [Si]=$2.8x10^{20}$ cm^{-3} was grown graded from $In_{0.07}Ga_{0.93}N$ at the bottom of the layer to GaN at the top of the layer. Then, a 6 nm n++GaN layer with [Si]=$2.8x10^{20}$ cm^{-3} was grown. These two n++(In)GaN layers form the n-side of the TJ. Next a 400nm thick n-GaN recovery layer was grown with [Si]=$5x10^{18}$ cm^{-3}.

Cascaded LED structures were fabricated starting with mesa-isolation of the device structure by Inductively Coupled Plasma - Reactive Ion Etching (ICP-RIE) etching followed by activation of buried p-GaN layers in a rapid thermal anneal system. The details of the buried p-GaN activation process are discussed in elsewhere.[24] Ti/Al/Ni/Au bottom n-type contact was evaporated and annealed for 30 seconds at 850°C in N_2 ambient. Ring-shaped Al/Ni/Au top n-type contacts were deposited and annealed for 2 minutes at 500°C in N_2 ambient.

The various structures were characterized electrically and optically. Current-voltage characteristics were measured on a Keysight B1500A semiconductor device analyzer. Electroluminescence measurements were performed using a linear silicon CCD array detector based spectrometer fitted with a cosine corrector to increase the collection field of view. The probe was positioned above each sample manually for each measurement and replication of the same geometry between subsequent measurements was difficult, as such, the intensities of the EL spectra should not be compared quantitatively. The measurement is accurate for determining the peak wavelength of the EL spectra. In order to calculate the EQE of the cascaded LED structures, the optical output power was measured using a Thorlabs PM100D optical power meter fitted with a S120VC photodiode power sensor. The devices were placed directly on top of the photodiode power sensor and probed from the top for

electrical contact. The light was collected from the backside of the sample through the sapphire substrate. The optical power measurements reported here are absolute values from the power meter and may therefore underestimate the output power since the measurements are done on-wafer without any device packaging.

Results

Electrical characterization of the LEDs shows excellent scaling in the forward turn-on voltage, with the lowest turn-on voltage reported to-date for MOCVD-grown 2-junction and 3-junction LEDs (Fig. 3). At 10 A/cm^2, the forward voltage drop for the 1/2/3 junction LEDs was 3.3V/6.9V/10.8V, representing a voltage increment of 210% for the 2-junction LED, and 330% for the 3-junction LED.

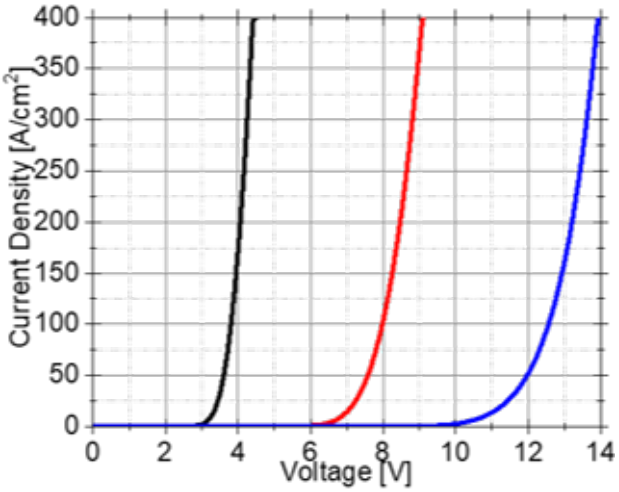

Fig. 3 The measured J-V characteristics of the single (black), dual (red), and triple (blue) junction devices.

These are significantly better than results reported earlier for MOCVD-grown cascaded LEDs for 2-junction LEDs (Table 1). The relative increase in the voltage for the 2- and 3-junction LEDs is suspected to be related to the thermal budget associated with the growth of the multiple active region structure.

Number of Junctions	Voltage Scaling	EQE Scaling	Reference
2	210%	200%	This Work (MOCVD)
3	330%	260%	This Work (MOCVD)
2	270%	173%	[17] (MOCVD)
2	306%	133%	[17] (MOCVD)
3	312%	N/A	[25] (MBE)

Table 1. This table shows the current state-of-the-art metrics for multi-active region III-Nitride LEDs. Comparisons of the voltage scaling, peak EQE scaling, and WPE scaling for dual and triple junction devices reported in this work, and in previous works.[17],[25]

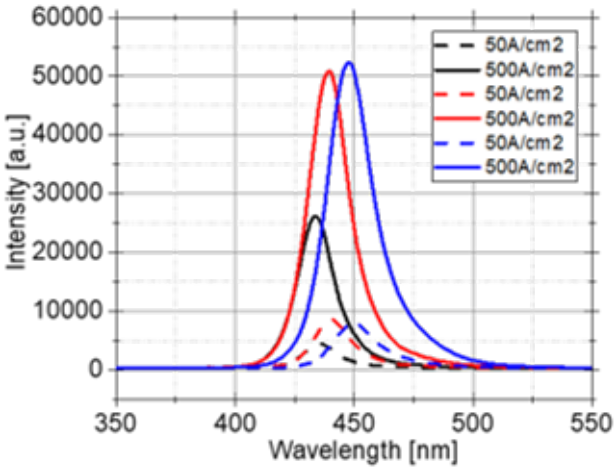

Fig. 4 The electroluminescence characteristics of the single (black), dual (red), and triple (blue) junction devices measured at 50 A/cm^2 (dashed) and 500 A/cm^2 (solid).

The devices were characterized on-wafer optically by electroluminescence (EL) measurements as described earlier. The EL peak shifts by ~ 6 nm for each additional junction, ranging from 436nm to 448nm as shown in Fig. 4. The EQE (output optical flux/input current) was measured and compared for all three devices (Fig. 5). The peak EQE scaled by 200% for the 2-junction device, and 260% for the 3-junction device. The scaling of external quantum efficiency demonstrates the benefit of multi-active region LED structures for high power density operation. The reduction in the EQE scaling for the 3-junction device is also suspected to be a result of thermal degradation of the bottom-most LED due to the thermal budget associated with growing the 3-junction structure.

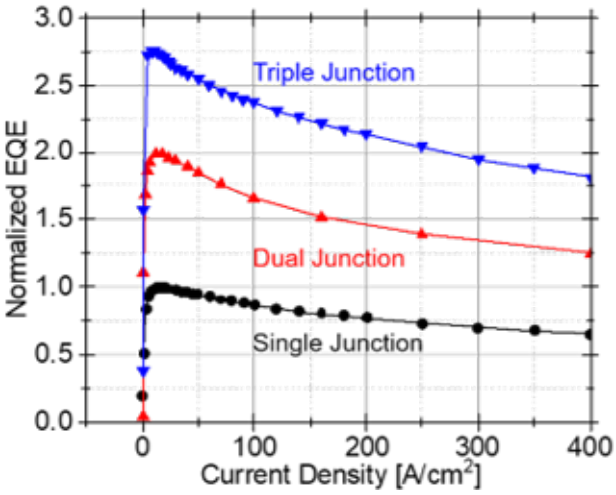

Fig. 5 The measured relative EQE of the single (black), dual (red), and triple (blue) junction devices.

The wall-plug efficiency was estimated for the devices (Fig. 6), and the WPE for the dual junction device was found to be greater than in the single junction device above a power density of 5 W/cm^2, while the WPE is greater in the triple junction device than in the dual or single junction device above 15 W/cm^2. The improvement in WPE with increasing output power shows that multi-active region devices can be operated at significantly higher power density while maintaining high efficiency compared with the single-junction LED. Table 1 compares 2 and 3-junction LEDs with previous multi-active region III-Nitride LEDs reports.[17,25] The results reported here show significant improvement in the voltage and EQE scaling compared with previous work and show that by utilizing proper TJ design the multi-junction cascaded LED approach is a promising approach for overcoming efficiency droop in high-power III-Nitride LEDs.

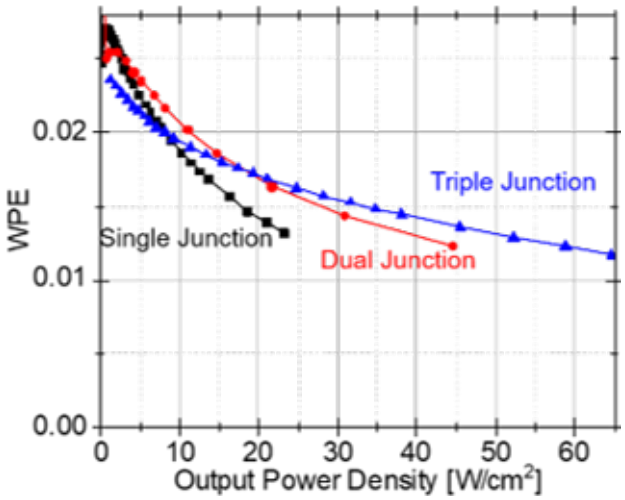

Fig. 6 The measured WPE as a function of output power for the single (black), dual (red), and triple (blue) junction devices.

In order to push the limits of the multi-active region device structure further, there are a few routes which may be explored. Further reduction in TJ forward voltage will improve WPE in the cascaded LED structures. Another means of improving the WPE in the cascaded LED structures for use in high-power LEDs is to increase the number of cascaded active regions in the structure. This would require a thorough investigation of thermal degradation in underlying LEDs within the multi-active region LED structures, as thermal budget is a significant limitation associated with the growth of multi-active region structures with a large number of junctions. Finally, the light extraction efficiency for multi-junction LEDs is also relatively unexplored. Future research on understanding the impact of spacing between active regions, losses in highly doped tunnel junction regions, and the impact of re-absorption would help to understand the optimal designs for future multiple active region LED devices.

Acknowledgements

This material is based upon work supported by the U.S. Department of Energy's Office of Energy Efficiency and Renewable Energy (EERE) under the Building Technologies Office (BTO) Award Number 31150. Sandia National Laboratories is a multi-mission laboratory managed and operated by National Technology and Engineering Solutions of Sandia, LLC., a wholly owned subsidiary of Honeywell International, Inc., for the U.S. Department of Energy's National Nuclear Security

Administration under contract DE-NA-0003525. The views expressed in the article do not necessarily represent the views of the U.S. Department of Energy or the United States Government.

Data Availability

Data available on request from the authors.

References

[1] Shigeya Kimura, Hisashi Yoshida, Kenjiro Uesugi, Toshihide Ito, Aoi Okada, and Shinya Nunoue, Journal of Applied Physics **120** (11), 113104 (2016).
[2] DOE Solid State Lighting Roadmap (2019).
[3] Min-Ho Kim, Martin F. Schubert, Qi Dai, Jong Kyu Kim, E. Fred Schubert, Joachim Piprek, and Yongjo Park, Applied Physics Letters **91** (18), 183507 (2007).
[4] Hongping Zhao, Guangyu Liu, Ronald A. Arif, and Nelson Tansu, Solid-State Electronics **54** (10), 1119 (2010).
[5] Fatih Akyol, Sriram Krishnamoorthy, and Siddharth Rajan, Applied Physics Letters **103** (8), 081107 (2013).
[6] Fatih Akyol, Yuewei Zhang, Sriram Krishnamoorthy, and Siddharth Rajan, Applied Physics Express **10** (12), 121003 (2017).
[7] Xiaodong Yan, Wenjun Li, S. M. Islam, Kasra Pourang, Huili Xing, Patrick Fay, and Debdeep Jena, Appl. Phys. Lett. **107** (16), 163504 (2015).
[8] Sriram Krishnamoorthy, Fatih Akyol, Pil Sung Park, and Siddharth Rajan, Applied Physics Letters **102** (11), 113503 (2013).
[9] SeungGeun Lee, Charles A. Forman, Changmin Lee, Jared Kearns, Erin C. Young, John T. Leonard, Daniel A. Cohen, James S. Speck, Shuji Nakamura, and Steven P. DenBaars, Applied Physics Express **11** (6), 062703 (2018).
[10] Abdullah I. Alhassan, Erin C. Young, Ahmed Y. Alyamani, Abdulrahman Albadri, Shuji Nakamura, Steven P. DenBaars, and James S. Speck, Applied Physics Express **11** (4), 042101 (2018).
[11] B. P. Yonkee, E. C. Young, S. P. DenBaars, S. Nakamura, and J. S. Speck, Appl. Phys. Lett. **109** (19), 191104 (2016).
[12] Erin C. Young, Benjamin P. Yonkee, Feng Wu, Sang Ho Oh, Steven P. DenBaars, Shuji Nakamura, and James S. Speck, Applied Physics Express **9** (2), 022102 (2016).
[13] Christian Kuhn, Luca Sulmoni, Martin Guttmann, Johannes Glaab, Norman Susilo, Tim Wernicke, Markus Weyers, and Michael Kneissl, Photon. Res. **7** (5), B7 (2019).
[14] S. Neugebauer, M. P. Hoffmann, H. Witte, J. Bläsing, A. Dadgar, A. Strittmatter, T. Niermann, M. Narodovitch, and M. Lehmann, Applied Physics Letters **110** (10), 102 (2017).
[15] Pirouz Sohi, Mauro Mosca, Yao Chen, Jean-Francois Carlin, and Nicolas Grandjean, Semiconductor Science and Technology **34** (2018).
[16] S. Chang, W. Lin, and C. Yu, IEEE Electron Device Letters **36** (4), 366 (2015).
[17] S. Chang, W. Lin, and W. Chen, IEEE Journal of Quantum Electronics **51** (8), 1 (2015).
[18] Zane Jamal-Eddine, Syed M. N. Hasan, Brendan Gunning, Hareesh Chandrasekar, Mary Crawford, Andrew Armstrong, Shamsul Arafin, and Siddharth Rajan, Applied Physics Letters **117** (5), 051103 (2020).
[19] Daichi Minamikawa, Masataka Ino, Shunsuke Kawai, Tetsuya Takeuchi, Satoshi Kamiyama, Motoaki Iwaya, and Isamu Akasaki, physica status solidi (b) **252** (5), 1127 (2015).
[20] David Hwang, Asad J. Mughal, Matthew S. Wong, Abdullah I. Alhassan, Shuji Nakamura, and Steven P. DenBaars, Applied Physics Express **11** (1), 012102 (2017).
[21] Panpan Li, Haojun Zhang, Hongjian Li, Yuewei Zhang, Yifan Yao, Nathan Palmquist, Mike Iza, James S. Speck, Shuji Nakamura, and Steven P. DenBaars, Semiconductor Science and Technology **35** (12), 125023 (2020).
[22] Zane Jamal-Eddine, Syed M. N. Hasan, Brendan Gunning, Hareesh Chandrasekar, Mary Crawford, Andrew Armstrong, Shamsul Arafin, and Siddharth Rajan, Applied Physics Letters **118** (5), 053503 (2021).

[23] C. Haller, J. F. Carlin, G. Jacopin, D. Martin, R. Butté, and N. Grandjean, Applied Physics Letters **111** (26), 262101 (2017).
[24] Syed M. N. Hasan, Brendan P. Gunning, Zane J.-Eddine, Hareesh Chandrasekar, Mary H. Crawford, Andrew Armstrong, Siddharth Rajan, and Shamsul Arafin, Journal of Physics D: Applied Physics **54** (15), 155103 (2021).
[25] Fatih Akyol, Sriram Krishnamoorthy, Yuewei Zhang, and Siddharth Rajan, Applied Physics Express **8** (8), 082103 (2015).